IEEE Access
Multidisciplinary | Rapid Review | Open Access Journal

Received 18 February 2023, accepted 14 March 2023, date of publication 22 March 2023, date of current version 4 April 2023.

Digital Object Identifier 10.1109/ACCESS.2023.3260188

RESEARCH ARTICLE

Hierarchical Flatness-Based Control for Velocity Trajectory Tracking of the "DC/DC Boost Converter–DC Motor" System Powered by Renewable Energy

RAMÓN SILVA-ORTIGOZA[1], (Member, IEEE), ALFREDO ROLDÁN-CABALLERO[2], EDUARDO HERNÁNDEZ-MÁRQUEZ[3], (Member, IEEE), ROGELIO ERNESTO GARCÍA-CHÁVEZ[1], MAGDALENA MARCIANO-MELCHOR[1], JOSÉ RAFAEL GARCÍA-SÁNCHEZ[4], AND GILBERTO SILVA-ORTIGOZA[5]

[1]Laboratorio de Mecatrónica y Energía Renovable, CIDETEC, Instituto Politécnico Nacional, Ciudad de México 07700, Mexico
[2]Unidad Profesional Interdisciplinaria de Ingeniería Campus Tlaxcala, Instituto Politécnico Nacional, Tlaxcala 90000, Mexico
[3]Departamento de Ingeniería Mecatrónica, Instituto Tecnológico Superior de Poza Rica, Tecnológico Nacional de México, Veracruz 93230, Mexico
[4]División de Ingeniería Mecatrónica, Tecnológico de Estudios Superiores de Huixquilucan, Tecnológico Nacional de México, Estado de México 52773, Mexico
[5]Facultad de Ciencias Físico Matemáticas, Benemérita Universidad Autónoma de Puebla, Puebla 72570, Mexico

Corresponding authors: Ramón Silva-Ortigoza (rsilvao@ipn.mx) and Alfredo Roldán-Caballero (aroldanc@ipn.mx)

This work was supported by the Instituto Politécnico Nacional, Mexico. The work of Ramón Silva-Ortigoza and Magdalena Marciano-Melchor was supported in part by the SNI-México and in part by the IPN programs EDI and SIBE. The work of Alfredo Roldán-Caballero, Eduardo Hernández-Márquez, José Rafael García-Sánchez, and Gilberto Silva-Ortigoza was supported by the SNI-México. The work of Rogelio Ernesto García-Chávez was supported by the CONACYT-México and BEIFI scholarships.

ABSTRACT In this investigation, a tracking control is designed for the angular velocity of the DC/DC Boost converter–DC motor system. To this end, the dynamics of the power supply, generated through a renewable energy power source, is considered in both the mathematical model and the designed control. This latter is proposed by using a two-level hierarchical approach, where the dynamics of the DC/DC Boost converter and the one associated with the DC motor not only are treated as two independent subsystems, but also they exploit their differential flatness property. For the DC/DC Boost converter, an alternative first-order mathematical model is obtained for designing the low-level voltage control. Whereas, the well known second order mathematical model of the DC motor is used for developing the high-level angular velocity control. The robustness and performance of the hierarchical tracking control are verified via realistic numerical simulations and experimental results by using Matlab-Simulink, a prototype of the system, the DS1104 board, and the renewable energy emulator TDK-Lambda G100-17. The results demonstrate and validate the effectiveness of the proposed approach.

INDEX TERMS DC/DC Boost converter, DC motor, differential flatness, renewable energy, robust control, solar energy.

I. INTRODUCTION

The DC motor is an electric machine with several applications [1]. Some of these are at industrial level (pumps, fans, robotics, automation), civilian (home appliances, ventilation, air conditioning), transportation (trains, electric vehicles, aircraft), and renewable energy (motor-generator pair system, solar pumps), among others. Related to industry applications, systems using a DC motor represent, on average, the 60% of electric consumption [2]. Because of this, the renewable energy turns out to be an interesting topic when is focused on feeding a motor. On the other hand, since power

The associate editor coordinating the review of this manuscript and approving it for publication was Cheng Qian.

electronics converters have a high efficiency when converting electric energy, their application for driving motors feeded by renewable energy power sources is an excellent choice [3], [4]. In this sense, relevant published papers related to the DC/DC power electronics converters connected with DC motors are [5], [6], [7], [8], [9], [10], [11], [12], [13], [14], [15], [16], [17], [18], [19], [20], [21], [22], [23], [24], [25], [26], [27], [28], [29], [30], [31], [32], [33], [34], [35], [36], [37], [38], [39], [40], [41], [42], [43], [44], [45], [46], [47], [48], [49], [50], [51], [52], [53], [54], [55], [56], [57], [58], [59], [60], [61], [62], [63], [64], [65], [66], [67], being the Buck [5], [6], [7], [8], [9], [10], [11], [12], [13], [14], [15], [16], [17], [18], [19], [20], [21], [22], [23], [24], [25], [26], [27], [28], [29], [30], [31], [32], [33], [34], [35], [36], [37], [38], [39], [40], [41], [42], [43], [44], [45], [46] and the Boost [47], [48], [49], [50], [51], [52], [53], [54], [55] topologies the most commonly used.

A. DC/DC BUCK CONVERTER AS A DRIVER FOR A DC MOTOR

The DC/DC Buck converter is the most utilized topology for driving both the unidirectional [5], [6], [7], [8], [9], [10], [11], [12], [13], [14], [15], [16], [17], [18], [19], [20], [21], [22], [23], [24], [25], [26], [27], [28], [29], [30], [31], [32], [33], [34], [35], [36], [37], [38], [39] and the bidirectional [40], [41], [42], [43], [44], [45], [46] angular velocity of a DC motor.

Related to the unidirectional rotation of the motor shaft, the mathematical model of the DC/DC Buck converter–DC motor system was proposed by Lyshevski in [5]. After this, several control laws have been reported for solving either the regulation or the tracking tasks. In this regard, the control algorithms recently published in specialized literature are commonly designed on the basis of a well known strategy. For example, a nonlinear control [5], a fuzzy logic controller along with a linear quadratic regulator [6], fractional order controls [7], [8], [9], and an affine controller [10], were based on the well known proportional-integral-derivative (PID) control. In a different direction, the zero average dynamics (ZAD) technique [11], [12], [13], [14], sliding modes with dynamic surface [15], a finite-time disturbance observer [16], a continuous nonsingular terminal [17], and three variations of sliding modes [18], are papers where sliding modes were used as the basis control. On the other hand, differential flatness proposals [19] and [20], differential flatness and PI plus sliding modes [21], and linear PI controllers [22], were designed based on a hierarchical approach. Whereas, a generalized proportional integral (GPI) observer control [23], a nonlinear control [24], a control in successive loops [25], and a robust flatness-based tracking control [26], were developed by considering the differential flatness property. Additionally, a neuronal control [27], neuro-adaptive backstepping controls [28], [29], and an adaptive neurofuzzy H-infinity control [30], were proposed by using the neural networks technique. Other controls for driving the angular velocity of the DC/DC Buck converter–DC motor system were based on disturbance rejection controllers with a GPI observer [31], [32], [33], resonant extended state observers [34], [35], exact tracking error dynamics passive output feedback (ETEDPOF) control [36], [37], fault detection by error-based global analytical redundancy relations [38], and output feedback discrete-time model predictive control [39].

Related to the bidirectional rotation of the motor shaft, different topologies of the DC/DC Buck converter have been introduced. One of these corresponds to the DC/DC Buck converter–inverter–DC motor, whose mathematical model was proposed and experimentally validated in [40]. In such a system, the tracking task was solved through a control based on the ETEDPOF methodology in [41], via the proposal of two controls based on differential flatness [42], and by means of an adaptive backstepping using sliding modes control [43]. Another designed topology was the full-bridge Buck inverter–DC motor presented in [44] along with its mathematical model and corresponding experimental validation, while a tracking control based on the ETEDPOF methodology was reported in [45]. Lastly, the bidirectional tracking task was also solved by driving a DC motor through a clamped diode multilevel DC/DC Buck converter in [46].

B. DC/DC BOOST CONVERTER AS A DRIVER FOR A DC MOTOR

Controls for driving the angular velocity of a DC motor by using a DC/DC Boost converter as the driver, can be classified depending on the rotation of the motor shaft. This is, unidirectional rotation [47], [48], [49], [50], [51], [52] and bidirectional one [53], [54], [55], [56]. Related to the unidirectional rotation, the literature reported passivity controls [47], non-linear controls [48], [49], [50], digital controllers [51], and a current control based on fuzzy logic [52]. Regarding the bidirectional rotation, a new topology of the DC/DC Boost converter–DC motor was proposed and its mathematical model was experimentally validated in [53]. Also, for this new topology, a passive control was designed in [54] and a differential flatness-based robust control was developed in [55]. Whereas, a procedure based on sum-of-squares optimization was presented in [56].

Other topologies where the trajectory tracking task has been solved on the DC motor shaft are the Buck-Boost [57], [58], [59], [60], [61], [62], Sepic [63], [64], Sepic and Ćuk [65], Ćuk [66], and the Luo topology [67].

C. DISCUSSION OF RELATED WORKS AND CONTRIBUTION

From the previous state-of-the-art review [5], [6], [7], [8], [9], [10], [11], [12], [13], [14], [15], [16], [17], [18], [19], [20], [21], [22], [23], [24], [25], [26], [27], [28], [29], [30], [31], [32], [33], [34], [35], [36], [37], [38], [39], [40], [41], [42], [43], [44], [45], [46], [47], [48], [49], [50], [51], [52], [53], [54], [55], [56], [57], [58], [59], [60], [61], [62], [63], [64], [65], [66], [67], it was observed that the angular

velocity of the DC motor shaft was driven through different DC/DC power converters topologies. In this direction, the corresponding topology is chosen depending on the application for the DC motor. Thus, the DC/DC Boost converter turns out to be an excellent choice when renewable energy power sources are going to be used. This, because the output of such a topology is equal or greater than the input voltage [68]. However, papers where the DC/DC Boost converter has been used as a driver for a DC motor [47], [48], [49], [50], [51], [52], [53], [54], [55], [56] did not use a renewable energy power source. On the other hand, works where a renewable energy power source was indeed used for the DC/DC power converter–DC motor system were devoted to the Buck [33], [43], Sepic [63], Sepic and Ćuk [65] topologies. Nevertheless, the dynamic associated with the renewable energy power source was neglected for control purposes.

From the aforementioned, this work presents a two-level hierarchical robust control that contemplates, for the first time, the dynamics of the renewable energy power source that feeds the system with the aim of solving the angular velocity tracking task in the DC/DC Boost converter–DC motor. The effectiveness and performance of the control are verified via realistic numerical simulations and through its experimental implementation. Both results show the accomplishment of the control task, i.e., $\omega \to \omega^*$, even when abrupt variations in parameters of the system are included.

The remaining of this paper is organized as follows. In Section II, generalities of the DC/DC Boost converter–DC motor system are given. In Section III, the high-level control and the low-level control are developed and then interconnected for generating the two-level hierarchical control. Section IV is devoted to simulation results, whereas Section V presents the corresponding experimental implementation of the proposed approach. Finally, Section VI concludes this paper and describes the future of this research.

II. DC/DC BOOST CONVERTER–DC MOTOR SYSTEM

In this investigation, the DC/DC Boost converter–DC motor system is considered to be the interconnection of two independently controlled subsystems, as can be observed in Fig. 1. On the one hand, the DC/DC Boost converter steps up the input voltage $E(t)$ depending on the input signal u with the aim of generating the output voltage υ. Here, an electric current i flows through the inductance L to be sent right to the parallel connection between the capacitor C and the load R in accordance with the operation of transistor Q and diode D. On the other hand, the angular velocity ω of the DC motor shaft is driven via the voltage ν. In this subsystem, the armature current i_a flows through the armature load R_a and the inductor L_a. The product between the pair constant k_m and i_a generates the torque of the motor. Since the armature rotates, an induced voltage is generated and corresponds to the product of the counter electromotive force k_e and the angular velocity ω. The remaining parameters are the moment of inertia J and the viscous friction coefficient of the motor shaft b.

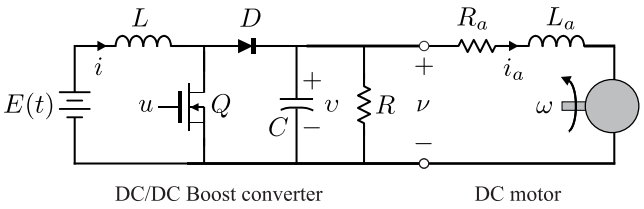

FIGURE 1. Subsystems DC/DC Boost converter and DC motor.

A. MATHEMATICAL MODELS OF THE DC/DC BOOST CONVERTER AND THE DC MOTOR

The mathematical model of the DC/DC Boost converter when the primary power supply is a renewable energy power source is given by [69]

$$\begin{aligned} L\frac{di}{dt} &= -(1-u_{av})\,\upsilon + E(t), \\ C\frac{d\upsilon}{dt} &= (1-u_{av})\,i - \frac{\upsilon}{R}. \end{aligned} \tag{1}$$

While the mathematical model of the DC motor is given by [21]

$$\begin{aligned} \frac{di_a}{dt} &= \frac{1}{L_a}\nu - \frac{k_e}{L_a}\omega - \frac{R_a}{L_a}i_a, \\ \frac{d\omega}{dt} &= -\frac{b}{J}\omega + \frac{k_m}{J}i_a. \end{aligned} \tag{2}$$

B. ALTERNATIVE FIRST-ORDER MATHEMATICAL MODEL FOR THE DC/DC BOOST CONVERTER

Since the dynamics associated with the model (1) is a non-minimum phase dynamics [70], for control purposes, this paper will use a reduced model for the DC/DC Boost converter. Such a model is achieved by approximating the second order dynamics (1) to a first order one by using an iterative process [70]. This process exploits the differential flatness property of (1), whose differential parametrization is

$$\begin{aligned} i &= -\frac{CE(t)R}{2L} + \gamma, \\ \upsilon &= \sqrt{\frac{2}{C}F - \frac{L}{C}\left(-\frac{CE(t)R}{2L} + \gamma\right)^2}, \\ u_{av} &= 1 - \frac{\dot{E}i + \frac{E(t)^2}{L} + \frac{2}{R^2C}\upsilon^2 - \ddot{F}}{\left(\frac{E(t)}{L} + \frac{2}{RC}i\right)\upsilon}, \end{aligned}$$

with

$$\gamma = \frac{1}{2}\sqrt{\left(\frac{RCE(t)}{L}\right)^2 + \frac{4}{L}\left(CR\dot{F} + 2F\right)},$$

and the flat output is given by

$$F = \frac{1}{2}Li^2 + \frac{1}{2}C\upsilon^2. \tag{3}$$

The iterative equations are found from the first derivative with respect to time of (3) and by using (1), so that the following is obtained

$$\dot{F} = E(t)i - \frac{1}{R}\upsilon^2,$$

and solving for the current i

$$i = \frac{\dot{F}}{E(t)} + \frac{1}{E(t)R}\upsilon^2. \tag{4}$$

From relation (4) and the flat output (3), the iterative process for obtaining the reduced model of (1) gives as a result

$$i_k = \frac{\dot{F}_k}{E(t)} + \frac{1}{E(t)R}\upsilon^2,$$
$$F_{k+1} = \frac{1}{2}Li_k^2 + \frac{1}{2}C\upsilon^2,$$

where $k \in \mathbb{N}$. This process generates a static relation between i and υ. It is worth mentioning that Hernández-Márquez et al. in [71] demonstrated that only one iteration is required for achieving a dynamic behavior similar to the one described by (1). From the first iteration, where F is considered to be constant, the following relation is obtained

$$i = \frac{1}{E(t)R}\upsilon^2. \tag{5}$$

Through the time derivative of (5), and by using (1), the following reduced model of first order is obtained for the DC/DC Boost converter that uses a renewable energy power source

$$\frac{d\upsilon}{dt} = \frac{R^2E^2(t)\left[-\left(1-u_{av}\right)\upsilon + E(t)\right] - RL\dot{E}(t)\upsilon^2}{2RLE(t)\upsilon}. \tag{6}$$

III. DESIGN OF THE HIERARCHICAL CONTROL BASED ON DIFFERENTIAL FLATNESS

The design of the two-level hierarchical control considers both the DC/DC Boost converter and the DC motor as independent subsystems, as depicted in Fig. 1. In this proposal, the low level corresponds to the control of the DC/DC Boost converter, whereas the high level is associated with the control of the DC motor.

A. LOW-LEVEL CONTROL

The low-level control is proposed by considering the reduced model of the DC/DC Boost converter (6). Note that in this model the input u_{av} can be represented as

$$u_{av} = 1 + \frac{RL\dot{E}(t)\upsilon + 2RLE(t)\dot{\upsilon}}{R^2E^2(t)} - \frac{E(t)}{\upsilon}. \tag{7}$$

Now, (7) is a convenient representation of the DC/DC Boost converter, since it will allow to define a suitable control over the voltage υ. Thus, the robustness of the low-level control will be reflected directly over the output voltage υ. In this manner, the two-level hierarchical control will be capable of compensating variations in this voltage so that the angular velocity tracking task be solved. Instead, if the dynamics (1) be used, with flat output $F = \frac{1}{2}\left(Li^2 + C\upsilon^2\right)$, a direct control over the voltage υ cannot be designed. After considering (7), the low-level control for the DC/DC Boost converter is proposed as follows

$$u_{av} = 1 + \frac{RL\dot{E}(t)\upsilon + 2RLE(t)\eta}{R^2E^2(t)} - \frac{E(t)}{\upsilon}, \tag{8}$$

where η is an auxiliary control given by

$$\eta = \dot{\upsilon}^* - \kappa_1\left(\upsilon - \upsilon^*\right) - \kappa_0\int_0^t\left(\upsilon - \upsilon^*\right)d\tau,$$

being κ_0 and κ_1 the gains of the control and υ^* the desired output voltage of the converter. After equating (7) with (8) and defining the tracking error as $e_b = \upsilon - \upsilon^*$, the error dynamics in closed-loop of the DC/DC Boost converter is

$$\ddot{e}_b + \kappa_1\dot{e}_b + \kappa_0 e_b = 0,$$

whose characteristic polynomial is defined as

$$P_b(s) = s^2 + \kappa_1 s + \kappa_0. \tag{9}$$

With the aim of achieving that $\upsilon \to \upsilon^*$, the polynomial (9) is equated with the following Hurwitz polynomial

$$P_{d_b} = s^2 + 2\zeta_b\omega_{n_b}s + \omega_{n_b}^2,$$

being ζ_b and ω_{n_b} the damping factor and the undamped natural frequency of the converter in closed-loop, respectively. Hence, the gains κ_0 and κ_1 of the low-level control are

$$\begin{aligned}\kappa_0 &= \omega_{n_b}^2,\\ \kappa_1 &= 2\zeta_b\omega_{n_b}.\end{aligned} \tag{10}$$

Note that the choice of ζ_b and ω_{n_b} for tuning the control will ensure that $e_b \to 0$ and, consequently, that $\upsilon \to \upsilon^*$ be achieved.

B. HIGH-LEVEL CONTROL

The high-level control, associated with the DC motor, exploits the differential flatness property of this subsystem. Such a control, in accordance with [21], is

$$\nu = \frac{JL_a}{k_m}\delta + \left(\frac{bL_a}{k_m} + \frac{JR_a}{k_m}\right)\dot{\omega} + \left(\frac{bR_a}{k_m} + k_e\right)\omega, \tag{11}$$

where the auxiliary control δ is proposed as

$$\delta = \ddot{\omega}^* - \alpha_2\left(\dot{\omega} - \dot{\omega}^*\right) - \alpha_1\left(\omega - \omega^*\right) - \alpha_0\int_0^t\left(\omega - \omega^*\right)d\tau,$$

where α_0, α_1, and α_2 are the control gains of the high-level control and ω^* is the desired angular velocity. Based on [21], the error dynamics in closed-loop is given by

$$\dddot{e}_m + \alpha_2\ddot{e}_m + \alpha_1\dot{e}_m + \alpha_0 e_m = 0,$$

with $e_m = \omega - \omega^*$ and whose characteristic polynomial is

$$P_m(s) = s^3 + \alpha_2 s^2 + \alpha_1 s + \alpha_0.$$

Similarly to the low-level control, the polynomial $P_m(s)$ is also equated with a Hurwitz one with the objective of carrying

out the tracking task. To this end, the Hurwitz polynomial for controlling the angular velocity ω is

$$P_{d_m}(s) = (s+a)\left(s^2 + 2\zeta_m\omega_{n_m}s + \omega_{n_m}^2\right),$$

being $0 < a$, ζ_m the damping factor and ω_{n_m} the undamped natural frequency of the DC motor in closed-loop. Thus, the gains of the high-level control are given as

$$\begin{aligned}\alpha_0 &= a\omega_{n_m}^2,\\ \alpha_1 &= \omega_{n_m}^2 + 2a\zeta_m\omega_{n_m},\\ \alpha_2 &= 2\zeta_m\omega_{n_m} + a,\end{aligned} \tag{12}$$

such that, after choosing the parameters a, ζ_m, and ω_{n_m}, the tracking task in this subsystem is performed, i.e., $\omega \to \omega^*$.

C. HIERARCHICAL CONTROL

With the intention of achieving that $\omega \to \omega^*$ through the high-level and low-level controls ν and u_{av}, respectively, the interconnection depicted in Fig. 2 must be realized. The high-level control accomplishes $\omega \to \omega^*$ through an appropriate voltage level ν feeding the DC motor. This voltage is generated by the low-level control when $\upsilon \to \upsilon^*$.

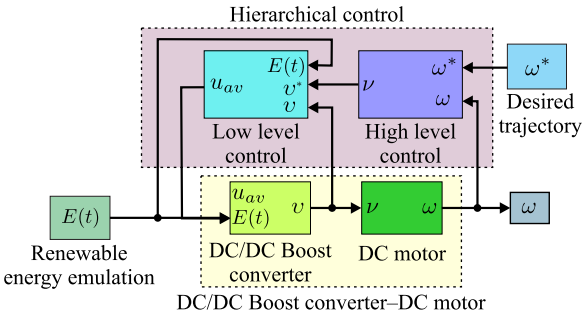

FIGURE 2. Block diagram of the DC/DC Boost converter–DC motor system in closed-loop.

After considering that the output voltage υ of the DC/DC Boost converter feeds the DC motor, it can be concluded the relation between both controls. This is, the desired voltage profile for the low-level control turns out to be the high-level control, i.e., $\upsilon^* = \nu$. Thus, the two-level hierarchical control is given by

$$u_{av} = \frac{RL\dot{E}(t)\upsilon + 2RLE(t)\left[\dot{\nu} - \kappa_1(\upsilon - \nu) - \kappa_0\int_0^t(\upsilon-\nu)\,d\tau\right]}{R^2E^2(t)} - \frac{E(t)}{\upsilon} + 1, \tag{13}$$

with ν, defined as

$$\nu = \frac{JL_a}{k_m}\left[\ddot{\omega}^* - \alpha_2\dot{e}_m - \alpha_1 e_m - \alpha_0\int_0^t e_m d\tau\right] + \left(\frac{bL_a}{k_m} + \frac{JR_a}{k_m}\right)\dot{\omega} + \left(\frac{bR_a}{k_m} + k_e\right)\omega.$$

IV. SIMULATION RESULTS OF THE HIERARCHICAL CONTROL

With the intention of verifying the performance of the two-level hierarchical control, four simulations were performed in Matlab-Simulink. The simulations consider the emulation of two renewable energy power sources and also perturbations in some parameters of the DC/DC Boost converter–DC motor. The following parameters, associated with the system in closed-loop, were used

$$\begin{aligned} &L = 4.94\text{ mH}, \quad C = 114.4\ \mu\text{F}, \quad R = 64\ \Omega,\\ &R_a = 0.965\ \Omega, \quad L_a = 2.22\text{ mH},\\ &k_m = 120.1\times10^{-3}\ \tfrac{\text{N·m}}{\text{A}}, \quad k_e = 120.1\times10^{-3}\ \tfrac{\text{V·s}}{\text{rad}},\\ &J = 118.2\times10^{-3}\ \text{kg·m}^2, \quad b = 129.6\times10^{-3}\ \tfrac{\text{N·m·s}}{\text{rad}}.\end{aligned}$$

Whereas, the desired angular velocity profile ω^* was proposed as a Bézier polynomial type given by

$$\omega^*(t) = \overline{\omega}_i(t_i) + [\overline{\omega}_f(t_f) - \overline{\omega}_i(t_i)]\lambda(t, t_i, t_f), \tag{14}$$

where $\overline{\omega}_i = 12\ \frac{\text{rad}}{\text{s}}$, $t_i = 4$ s, $\overline{\omega}_f = 15\ \frac{\text{rad}}{\text{s}}$, $t_f = 7$ s, and $\lambda(t, t_i, t_f)$ is defined as

$$\lambda\left(t, t_i, t_f\right) = \begin{cases} 0 & t \le t_i,\\ \left(\frac{t-t_i}{t_f-t_i}\right)^3 \times \left[20 - 45\left(\frac{t-t_i}{t_f-t_i}\right)\right. & \\ \left. +36\left(\frac{t-t_i}{t_f-t_i}\right)^2 - 10\left(\frac{t-t_i}{t_f-t_i}\right)^3\right] & t \in (t_i, t_f),\\ 1 & t \ge t_f. \end{cases} \tag{15}$$

The control gains are obtained after substituting the following values in (10) and (12)

$$\begin{aligned} &\omega_{n_m} = 500, \quad \zeta_m = 2.5, \quad a = 0.2,\\ &\omega_{n_b} = 50, \quad \zeta_b = 2.2.\end{aligned}$$

1) SIMULATION 1: DC/DC BOOST CONVERTER–DC MOTOR IN CLOSED-LOOP AND TIME-VARYING POWER SUPPLY WITH PERTURBATIONS IN LOAD R

The first simulation of the DC/DC Boost converter–DC motor system in closed-loop is shown in Fig. 3. In this result, the waveform for the voltage delivered by the power supply was proposed by Gil-Antonio et al. in [69]. This kind of waveform is very similar to the one rendered by a renewable energy power source. In this case, the waveform is defined by the following function

$$E(t) = 18 + 0.5504\sin(5t) + 0.5848\sin(10t). \tag{16}$$

Also, for this simulation, the following abrupt variations in load R were considered

$$R_p = \begin{cases} R & 0\text{ s} \le t < 3\text{ s},\\ 200\%R & 3\text{ s} \le t < 5\text{ s},\\ R & 5\text{ s} \le t < 8\text{ s},\\ 60\%R & 8\text{ s} \le t < 10\text{ s}. \end{cases} \tag{17}$$

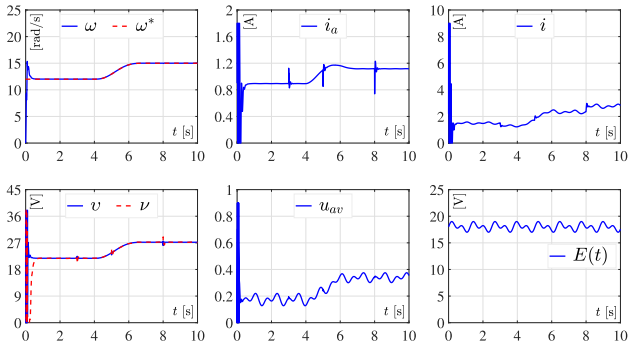

FIGURE 3. Dynamic response of the DC/DC Boost converter–DC motor system in closed-loop with the two-level hierarchical control (13) considering the time-varying power supply (16) and the load perturbations in R (17).

2) SIMULATION 2: DC/DC BOOST CONVERTER–DC MOTOR IN CLOSED-LOOP AND TIME-VARYING POWER SUPPLY WITH PERTURBATIONS IN C

The second simulation result, depicted in Fig. 4, takes into account, again, the same function for generating the voltage waveform delivered by the power supply, i.e., the form (16). In this case, abrupt variations were introduced into the capacitor C as follows

$$C_p = \begin{cases} C & 0\text{ s} \leq t < 3\text{ s}, \\ 200\%C & 3\text{ s} \leq t < 5\text{ s}, \\ C & 5\text{ s} \leq t < 8\text{ s}, \\ 50\%C & 8\text{ s} \leq t < 10\text{ s}. \end{cases} \tag{18}$$

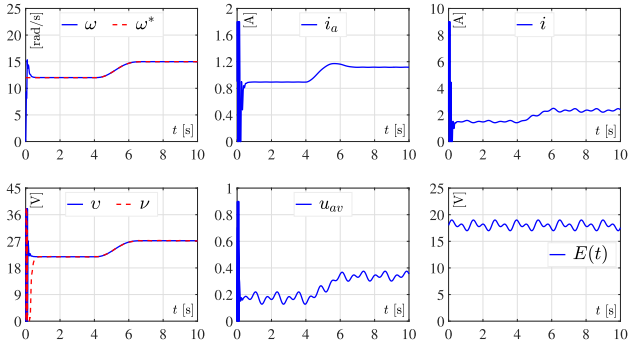

FIGURE 4. Dynamic behavior of the DC/DC Boost converter–DC motor system in closed-loop with the two-level hierarchical control (13) considering the time-varying power supply (16) and abrupt changes in capacitor C (18).

3) SIMULATION 3: DC/DC BOOST CONVERTER–DC MOTOR IN CLOSED-LOOP AND EMULATION OF A SOLAR PANEL AS THE POWER SUPPLY WITH PERTURBATIONS IN LOAD R

Unlike the first two simulations, the third simulation shown in Fig. 5 uses a waveform similar to the one generated by a solar panel with constant irradiance, as those described in [72] and [73]. The equation describing such a waveform is given by

$$E(t) = 21(1 - e^{-30t}) + 0.5\sin(100t) + 0.001. \tag{19}$$

For this simulation the perturbations were introduced over the load R and are described by (17).

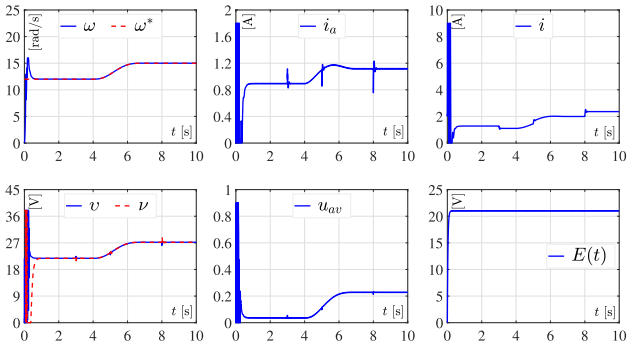

FIGURE 5. Dynamic response of the DC/DC Boost converter–DC motor in closed-loop with the two-level hierarchical control (13) considering a voltage waveform emerging from solar panels (19) and perturbations in load R (17).

4) SIMULATION 4: DC/DC BOOST CONVERTER–DC MOTOR IN CLOSED-LOOP AND EMULATION OF A SOLAR PANEL AS THE POWER SUPPLY WITH PERTURBATIONS IN C

The fourth simulation, presented in Fig. 6, introduces the abrupt changes (18) in capacitor C. This result also uses the power supply generated through (19).

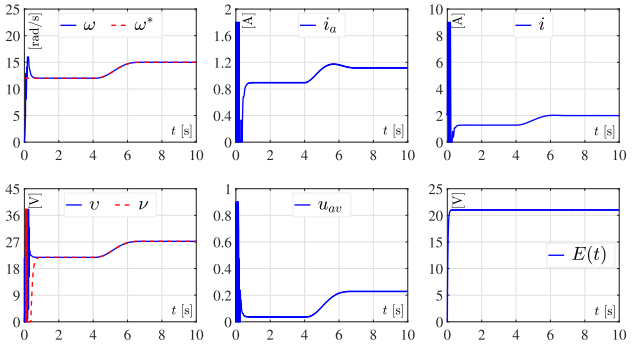

FIGURE 6. Dynamic behavior of the DC/DC Boost converter–DC motor in closed-loop with the two-level hierarchical control (13) considering a voltage waveform emerging from solar panels (19) and perturbations in C (18).

A. DISCUSSION ON THE SIMULATION RESULTS

As can be observed in Figs. 3–6, the tracking task is appropriately performed, since $\omega \to \omega^*$; meaning that also $\upsilon \to \upsilon^*$ even when abrupt changes in parameters of the system are introduced. It is worth noting, in such results, that in $t = 0$ s the desired angular velocity profile is different from 0 rad/s. This is due to the output voltage, υ, of the DC/DC Boost converter lies in the semi open interval $[E(t), \infty)$.

On the other hand, the influence of abrupt variations in load R (see Figs. 3 and 5) is greater than the one associated with the abrupt changes in capacitance C (see Figs. 4 and 6). This, because the former increases (or decreases) the consumption of current i; whereas, the latter affects the voltage ripple.

V. EXPERIMENTAL RESULTS OF THE HIERARCHICAL CONTROL

In this section, the experimental implementation of the two-level hierarchical control in closed-loop over a platform of the DC/DC Boost converter–DC motor system, is carried out.

In this direction, the experimental testbed is firstly described and then the obtained results are presented. The experiments contemplate a time-varying power supply $E(t)$ and the abrupt variations (17) and (18) for parameters R and C, respectively.

A. EXPERIMENTAL TESTBED OF THE DC/DC BOOST CONVERTER–DC MOTOR SYSTEM

In the following, the testbed for executing the two-level hierarchical control implementation is detailed. The experimental setup along with all the required elements are shown in the blocks of Fig. 7. These blocks are described next.

- *Renewable energy emulation*. This block shows the G100-17 TDK-Lambda power supply that emulates a renewable energy power source. This power supply is useful for obtaining several DC voltage waveforms by programming the required behavior. Also, this device allows to simulate solar panels. In addition, in this block the power supply voltage, $E(t)$, is measured via a Tektronix P5200A voltage probe.
- *DC/DC Boost converter–DC motor*. Here, the DC/DC Boost converter–DC motor prototype is depicted. The electric signals are acquired through a couple of Tektronix A622 current probes, for measuring i and i_a, a Tektronix P5200A voltage probe, for measuring υ, and an Omron E6B2-CWZ6C encoder for measuring the angular position θ. The parameters related to the system are defined in this block and, for the subsystem DC/DC Boost converter, are given by

$$L = 9.94 \text{ mH}, \qquad C = 114.4\ \mu\text{F}, \qquad R = 64\ \Omega.$$

  Whereas, the parameters of the DC motor, manufactured by Engel and gearbox GNM 5440-G3.1 with relation rate 14:1, are [74]

$$R_a = 0.965\ \Omega, \qquad L_a = 2.22 \text{ mH},$$
$$k_m = 120.1 \times 10^{-3}\ \frac{\text{N·m}}{\text{A}}, \qquad k_e = 120.1 \times 10^{-3}\ \frac{\text{V·s}}{\text{rad}},$$
$$J = 118.2 \times 10^{-3}\ \text{kg·m}^2, \qquad b = 129.6 \times 10^{-3}\ \frac{\text{N·m·s}}{\text{rad}}.$$

- *Data acquisition board and conditioning circuit*. The interconnection between the DC/DC Boost converter–DC motor prototype and Matlab-Simulink, via the DS1104 data acquisition board, is performed here. As can be observed, the required signals are treated through a conditioning block (SC) so that the control u be correctly processed and generated. Note that a TLP250 optocoupler is used for electric isolation between the acquisition board and the system.
- *Desired trajectory*. The desired angular velocity profile ω^* is programmed in this block, by using Matlab-Simulink, and is proposed as

$$\omega^*(t) = \overline{\omega}_i\,(t_i) + [\overline{\omega}_f(t_f) - \overline{\omega}_i\,(t_i)]\lambda(t, t_i, t_f), \qquad (20)$$

  where $\overline{\omega}_i = 12\ \frac{\text{rad}}{\text{s}}$, $t_i = 4$ s, $\overline{\omega}_f = 15\ \frac{\text{rad}}{\text{s}}$, $t_f = 7$ s, and $\lambda(t, t_i, t_f)$ defined in (15).
- *Hierarchical control*. This block contains the programming of the two-level hierarchical control (13) in Matlab-Simulink, i.e., the low-level control (8) and the high-level control (11) with the aim of achieving that $\omega \to \omega^*$.

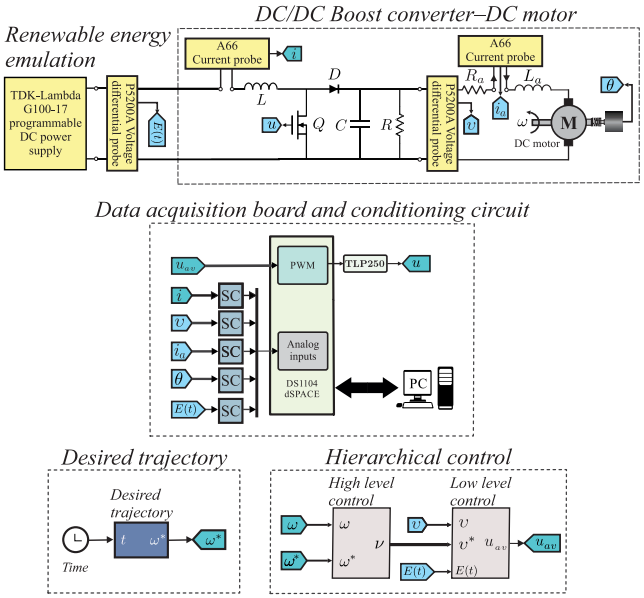

FIGURE 7. Experimental platform of the DC/DC Boost converter–DC motor system.

B. EXPERIMENTAL RESULTS

The experimental results of the DC/DC Boost converter–DC motor system in closed-loop are presented here. The experiments were performed in correspondence with the simulations of Section IV; thus, four experiments were executed. In this regard, the first two experiments consider as the voltage waveform the proposed function reported in (16) (which emulates a renewable energy power source). This function is generated through programming the TDK-Lambda G100-17 power supply. The other two experiments contemplate, as the power supply, the voltage waveform (19), corresponding to the waveform delivered by solar panel Ameresco Solar LLC 50 J – 50 W. This waveform is generated through the solar panel simulation-module of the TDK-Lambda G100-17 power supply by introducing the parameters, given by the manufacturer of the solar panel, shown in Fig. 8.

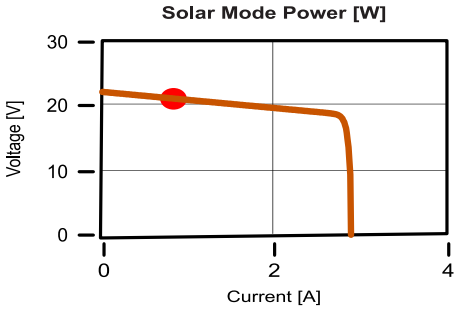

FIGURE 8. *V – I* graphic associated with the emulation of the solar panel Ameresco Solar LLC 50 J – 50 W, generated through the TDK-Lambda G100-17 power supply and corresponding to *E(t)*.

The desired angular velocity profile ω^* is proposed via the Bézier polynomial (20), while the gains (10) and (12) of the two-level hierarchial control (13) are calculated by using the following values

$$\omega_{n_m} = 60, \qquad \zeta_m = 6, \qquad a = 4,$$
$$\omega_{n_b} = 100, \qquad \zeta_b = 50.$$

1) EXPERIMENT 1: DC/DC BOOST CONVERTER–DC MOTOR IN CLOSED-LOOP AND TIME-VARYING POWER SUPPLY WITH PERTURBATIONS IN LOAD R

The first experiment corresponds to simulation 1 and is depicted in Fig. 9. Here, the waveform implemented for the power supply is (16). Also, abrupt changes in load R are introduced and are given by

$$R_p = \begin{cases} R & 0\text{ s} \leq t < 3\text{ s}, \\ 200\%R & 3\text{ s} \leq t < 5\text{ s}, \\ R & 5\text{ s} \leq t < 8\text{ s}, \\ 60\%R & 8\text{ s} \leq t < 10\text{ s}. \end{cases} \tag{21}$$

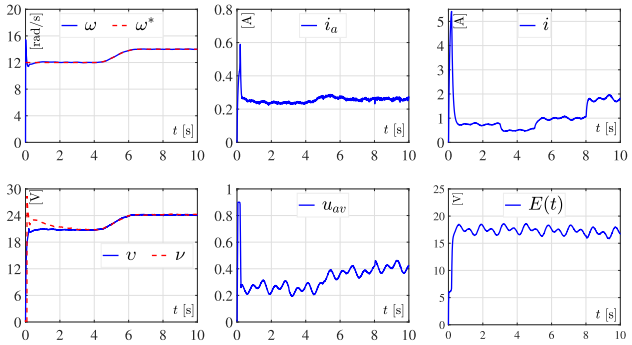

FIGURE 9. Experiment of the DC/DC Boost converter–DC motor system in closed-loop with the two-level hierarchical control (13) considering the waveform (16) for the power supply and perturbations (21) for load R.

2) EXPERIMENT 2: DC/DC BOOST CONVERTER–DC MOTOR IN CLOSED-LOOP AND TIME-VARYING POWER SUPPLY WITH PERTURBATIONS IN CAPACITANCE C

The second experiment, analogue to simulation 2, uses the time-varying power supply $E(t)$ described by (16). Now, abrupt variations in capacitance C are considered and are described by

$$C_p = \begin{cases} C & 0\text{ s} \leq t < 3\text{ s}, \\ 200\%C & 3\text{ s} \leq t < 5\text{ s}, \\ C & 5\text{ s} \leq t < 8\text{ s}, \\ 50\%C & 7\text{ s} \leq t < 10\text{ s}. \end{cases} \tag{22}$$

The experimental results for this experiment are shown in Fig. 10.

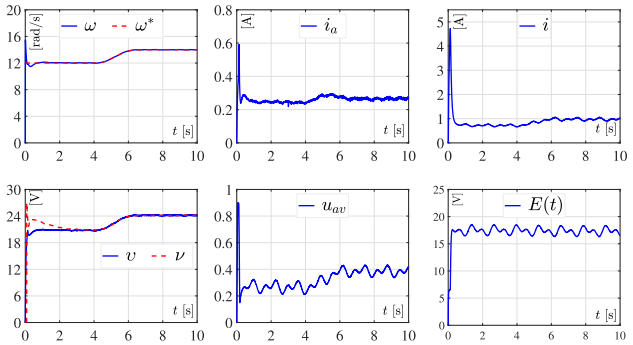

FIGURE 10. Experiment of the DC/DC Boost converter–DC motor system in closed-loop with the two-level hierarchical control (13) considering the time-varying waveform (16) for the power supply and perturbations (22) for capacitance C.

3) EXPERIMENT 3: DC/DC BOOST CONVERTER–DC MOTOR IN CLOSED-LOOP AND EMULATION OF A SOLAR PANEL AS THE POWER SUPPLY WITH PERTURBATIONS IN LOAD R

Experiment 3 is the counterpart of simulation 3 and is plotted in Fig. 11. The power supply corresponds to the emulation of the solar panel Ameresco Solar LLC 50 J − 50 W (19) through the TDK-Lambda G100-17. In addition, the abrupt variations given by (21) for load R are also taken into account.

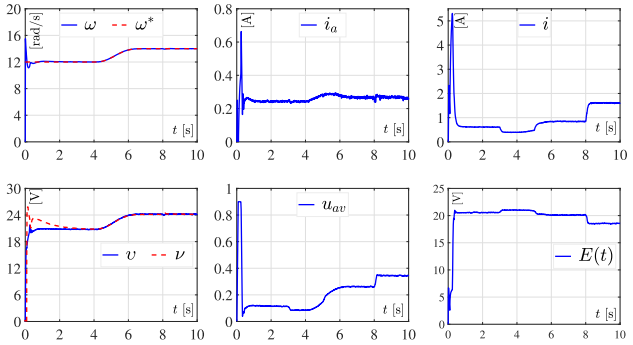

FIGURE 11. Experimental behavior of the DC/DC Boost converter–DC motor system in closed-loop with the two-level hierarchical control (13) considering the emulation of solar panel Ameresco Solar LLC 50 J – 50 W (19) as the power supply and perturbations (21) for load R.

4) EXPERIMENT 4: DC/DC BOOST CONVERTER–DC MOTOR IN CLOSED-LOOP AND EMULATION OF A SOLAR PANEL AS THE POWER SUPPLY WITH PERTURBATIONS IN CAPACITANCE C

This last experiment is analogue to simulation 4 and is depicted in Fig. 12. This experiment considers, similar to the previous one, the emulation of solar panel Ameresco Solar LLC 50 J − 50 W (19), as the power supply, through the TDK-Lambda G100-17. In this case, the abrupt variations in capacitance C (22) were introduced.

C. DISCUSSION OF THE EXPERIMENTAL RESULTS

The experimental results of the DC/DC Boost converter–DC motor in closed-loop presented in Figs. 9–12 demonstrated the effectiveness of the proposed two-level hierarchical control (13), since was achieved that $\upsilon \rightarrow \upsilon^*$ and,

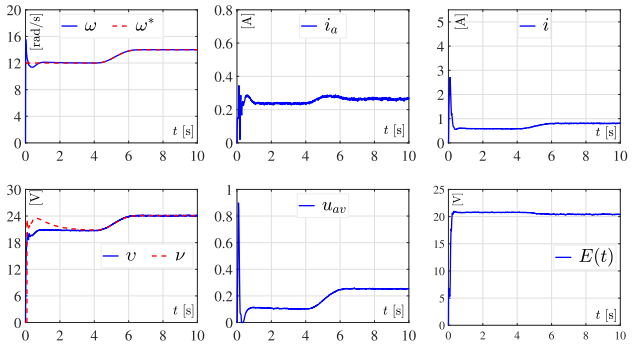

FIGURE 12. Experimental behavior of the DC/DC Boost converter–DC motor system in closed-loop with the two-level hierarchical control (13) considering the emulation of solar panel Ameresco Solar LLC 50 J – 50 W as the power supply and perturbations (22) for capacitance C.

consequently, $\omega \rightarrow \omega^*$. Regarding the experiments of Figs. 9 and 10, these were carried out when the waveform (16), associated with a renewable energy power source, was used as the power supply. Note that the control objective $\omega \rightarrow \omega^*$ was accomplished even when natural sinusoids-alike variations over the waveform $E(t)$ emerged. Related to the experiments of Figs. 11 and 12, these were obtained by using the waveform (19) as the power supply, via TDK-Lambda G100-17, and corresponds to the emulation of solar panel Ameresco Solar LLC 50 J − 50 W. Here, $E(t)$ slowly drops when the current i rises. Such a behavior is due to the solar panel, whose electric relation $V - I$ is plotted in Fig. 8. However, the average control u_{av} compensates those variations and, thus, the control objective is again achieved, i.e., $\omega \rightarrow \omega^*$. Additionally, the robustness of the control (13) was demonstrated after introducing abrupt variations in some parameters of the DC/DC Boost converter–DC motor system. On the one hand, load perturbations R were considered and the flowing current i was directly affected, as can be seen in Figs. 9 and 11. On the other hand, variations in capacitance C were also contemplated and the voltage ripple was slightly affected, as shown in Figs. 10 and 12. Nevertheless, and despite all those changes, the control objective was performed at each instant of time, i.e., $\omega \rightarrow \omega^*$.

VI. CONCLUSION

This paper presents, for the first time in literature, a robust hierarchical control that takes into account the dynamics of a renewable energy power source in its design for solving the angular velocity trajectory tracking task in the DC/DC Boost converter–DC motor system. The control considers two levels, a higher and a lower, each one for independently control the subsystems that compose the whole system, i.e., the DC Boost converter and the DC motor. The low-level control, associated with the DC/DC Boost converter, exploits the differential flatness property related to the first order mathematical model of the converter and uses the dynamics of the power supply $E(t)$. This control is capable of achieving that $\upsilon \rightarrow \upsilon^*$. Whereas, the high-level control also uses the differential flatness property but now the one of the DC motor for performing the angular velocity tracking task, i.e., $\omega \rightarrow \omega^*$. Then, both controls were interconnected in order to work as a whole and, thus, to generate the two-level hierarchical control. Note that, due to the control design, any kind of time-varying power supply can be used without the need of redesigning the control approach. The effectiveness and performance of the proposed control were verified through numerical simulations and by implementing the control on an experimental platform of the system. Abrupt variations were considered in some parameters of the system with the aim of verifying the robustness of the two-level hierarchical control in closed-loop.

Motivated by the obtained results, future work will be focused on considering abrupt changes in other parameters of the system so that the robustness of the proposed approach be verified through simulation and experimental results. Also, the DC/DC Boost converter–DC motor system along with the two-level hierarchical control will be implemented on a mobile robot, where a solar panel will be used as the primary power supply.

REFERENCES

[1] J. F. Gieras, *Permanent Magnet Motor Technology: Design and Applications*, 3rd ed. Boca Raton, FL, USA: CRC Press, 2010.
[2] S.-M. Lu, "A review of high-efficiency motors: Specification, policy, and technology," *Renew. Sustain. Energy Rev.*, vol. 59, pp. 1–12, Jun. 2016, doi: 10.1016/j.rser.2015.12.360.
[3] M. A. Hannan, M. S. H. Lipu, P. J. Ker, R. A. Begum, V. G. Agelidis, and F. Blaabjerg, "Power electronics contribution to renewable energy conversion addressing emission reduction: Applications, issues, and recommendations," *Appl. Energy*, vol. 251, Oct. 2019, Art. no. 113404, doi: 10.1016/j.apenergy.2019.113404.
[4] K. V. G. Raghavendra, K. Zeb, A. Muthusamy, T. N. V. Krishna, S. V. S. V. P. Kumar, D.-H. Kim, M.-S. Kim, H.-G. Cho, and H.-J. Kim, "A comprehensive review of DC–DC converter topologies and modulation strategies with recent advances in solar photovoltaic systems," *Electron.*, vol. 9, no. 1, pp. 1–41, 2020, doi: 10.3390/electronics9010031.
[5] S. E. Lyshevski, *Electromechanical Systems, Electric Machines, and Applied Mechatronics*. Boca Raton, FL, USA: CRC Press, 1999.
[6] M. A. Ahmad, R. M. T. Raja Ismail, and M. S. Ramli, "Control strategy of Buck converter driven DC motor: A comparative assessment," *Austral. J. Basic Appl. Sci.*, vol. 4, no. 10, pp. 4893–4903, 2010. [Online]. Available: http://www.ajbasweb.com/old/ajbas/2010/4893-4903.pdf
[7] S. Khubalkar, A. Chopade, A. Junghare, M. Aware, and S. Das, "Design and realization of stand-alone digital fractional order PID controller for Buck converter fed DC motor," *Circuits, Syst., Signal Process.*, vol. 35, no. 6, pp. 2189–2211, 2016.
[8] S. W. Khubalkar, A. S. Junghare, M. V. Aware, A. S. Chopade, and S. Das, "Demonstrative fractional order–PID controller based DC motor drive on digital platform," *ISA Trans.*, vol. 82, pp. 79–93, Nov. 2018.
[9] M. D. Patil, K. Vadirajacharya, and S. W. Khubalkar, "Design and tuning of digital fractional-order PID controller for permanent magnet DC motor," *IETE J. Res.*, pp. 1–11, Jun. 2021, doi: 10.1080/03772063.2021.1942243.
[10] M. I. F. M. Hanif, M. H. Suid, and M. A. Ahmad, "A piecewise affine PI controller for Buck converter generated DC motor," *Int. J. Power Electron. Drive Syst.*, vol. 10, no. 3, pp. 1419–1426, Sep. 2019. [Online]. Available: http://ijpeds.iaescore.com/index.php/IJPEDS/article/view/19852/12866
[11] F. E. Hoyos, A. Rincón, J. A. Taborda, N. Toro, and F. Angulo, "Adaptive quasi-sliding mode control for permanent magnet DC motor," *Math. Problems Eng.*, vol. 2013, Nov. 2013, Art. no. 693685. [Online]. Available: https://www.hindawi.com/journals/mpe/2013/693685
[12] F. E. Hoyos Velasco, J. E. Candelo-Becerra, and A. Rincón-Santamaría, "Dynamic analysis of a permanent magnet DC motor using a Buck converter controlled by ZAD-FPIC," *Energies*, vol. 11, no. 12, 2018, Art. no. 3388. [Online]. Available: https://www.mdpi.com/1996-1073/11/12/3388
[13] F. E. Hoyos, J. E. Candelo-Becerra, and C. I. Hoyos Velasco, "Application of zero average dynamics and fixed point induction control techniques to control the speed of a DC motor with a Buck converter," *Appl. Sci.*, vol. 10, no. 5, Mar. 2020, Art. no. 1807.

[14] F. E. Hoyos, J. E. Candelo-Becerra, and A. Rincón, "Zero average dynamic controller for speed control of DC motor," *Appl. Sci.*, vol. 11, no. 12, Jun. 2021, Art. no. 5608, doi: 10.3390/app11125608.

[15] F. Wei, P. Yang, and W. Li, "Robust adaptive control of DC motor system fed by Buck converter," *Int. J. Control Autom.*, vol. 7, no. 10, pp. 179–190, 2014, doi: 10.14257/ijca.2014.7.10.17.

[16] A. Rauf, S. Li, R. Madonski, and J. Yang, "Continuous dynamic sliding mode control of converter-fed DC motor system with high order mismatched disturbance compensation," *Trans. Inst. Meas. Control*, vol. 42, no. 14, pp. 2812–2821, Oct. 2020.

[17] A. Rauf, M. Zafran, A. Khan, and A. R. Tariq, "Finite-time nonsingular terminal sliding mode control of converter-driven DC motor system subject to unmatched disturbances," *Int. Trans. Elect. Energy Syst.*, vol. 2021, Aug. 2021, Art. no. e13070, doi: 10.1002/2050-7038.13070.

[18] D. Ravikumar and G. K. Srinivasan, "Implementation of higher order sliding mode control of DC–DC Buck converter fed permanent magnet DC motor with improved performance," *Automatika*, vol. 64, no. 1, pp. 162–177, 2023, doi: 10.1080/00051144.2022.2119499.

[19] R. Silva-Ortigoza, J. R. García-Sánchez, J. M. Alba-Martínez, V. M. Hernández-Guzmán, M. Marcelino-Aranda, H. Taud, and R. Bautista-Quintero, "Two-stage control design of a Buck converter/DC motor system without velocity measurements via a $\Sigma - \Delta$-modulator," *Math. Problems Eng.*, vol. 2013, Jun. 2013, Art. no. 929316. [Online]. Available: https://www.hindawi.com/journals/mpe/2013/929316

[20] R. Silva-Ortigoza, C. Márquez-Sánchez, F. Carrizosa-Corral, M. Antonio-Cruz, J. M. Alba-Martínez, and G. Saldaña-González, "Hierarchical velocity control based on differential flatness for a DC/DC Buck converter-DC motor system," *Math. Problems Eng.*, vol. 2014, Apr. 2014, Art. no. 912815. [Online]. Available: https://www.hindawi.com/journals/mpe/2014/912815

[21] R. Silva-Ortigoza, V. M. Hernández-Guzmán, M. Antonio-Cruz, and D. Muñoz-Carrillo, "DC/DC Buck power converter as a smooth starter for a DC motor based on a hierarchical control," *IEEE Trans. Power Electron.*, vol. 30, no. 2, pp. 1076–1084, Feb. 2015. [Online]. Available: http://ieeexplore.ieee.org/document/6767144

[22] V. M. Hernández-Guzmán, R. Silva-Ortigoza, and D. Muñoz-Carrillo, "Velocity control of a brushed DC-motor driven by a DC to DC Buck power converter," *Int. J. Innov. Comput., Inf. Control*, vol. 11, no. 2, pp. 509–521, 2015. [Online]. Available: http://www.ijicic.org/ijicic-110209.pdf

[23] H. Sira-Ramírez and M. A. Oliver-Salazar, "On the robust control of Buck-converter DC-motor combinations," *IEEE Trans. Power Electron.*, vol. 28, no. 8, pp. 3912–3922, Aug. 2013, doi: 10.1109/TPEL.2012.2227806.

[24] G. Rigatos, P. Siano, P. Wira, and M. Sayed-Mouchaweh, "Control of DC–DC converter and DC motor dynamics using differential flatness theory," *Intell. Ind. Syst.*, vol. 2, no. 4, pp. 371–380, 2016. [Online]. Available: https://link.springer.com/article/10.1007/s40903-016-0061-x

[25] G. Rigatos, P. Siano, S. Ademi, and P. Wira, "Flatness-based control of DC–DC converters implemented in successive loops," *Electr. Power Compon. Syst.*, vol. 46, no. 6, pp. 673–687, 2018, doi: 10.1080/15325008.2018.1464612.

[26] R. Silva-Ortigoza, A. Roldán-Caballero, E. Hernández-Márquez, J. R. García-Sánchez, M. Marciano-Melchor, V. M. Hernández-Guzmán, and G. Silva-Ortigoza, "Robust flatness tracking control for the 'DC/DC Buck converter-DC motor' system: Renewable energy-based power supply," *Complexity*, vol. 2021, Oct. 2021, Art. no. 2158782, doi: 10.1155/2021/2158782.

[27] O. Bingöl and S. Paçaci, "A virtual laboratory for neural network controlled DC motors based on a DC–DC Buck converter," *Int. J. Eng. Educ.*, vol. 28, no. 3, pp. 713–723, 2012.

[28] T. K. Nizami, A. Chakravarty, and C. Mahanta, "Design and implementation of a neuro-adaptive backstepping controller for Buck converter fed PMDC-motor," *Control Eng. Pract.*, vol. 58, pp. 78–87, Jan. 2017.

[29] T. K. Nizami, A. Chakravarty, C. Mahanta, A. Iqbal, and A. Hosseinpour, "Enhanced dynamic performance in DC–DC converter-PMDC motor combination through an intelligent non-linear adaptive control scheme," *IET Power Electron.*, vol. 15, no. 15, pp. 1607–1616, 2022, doi: 10.1049/pel2.12330.

[30] G. Rigatos, P. Siano, and M. Sayed-Mouchaweh, "Adaptive neurofuzzy H-infinity control of DC–DC voltage converters," *Neural Comput. Appl.*, vol. 32, no. 7, pp. 2507–2520, 2020.

[31] E. Guerrero, E. Guzmán, J. Linares, A. Martínez, and G. Guerrero, "FPGA-based active disturbance rejection velocity control for a parallel DC/DC Buck converter-DC motor system," *IET Power Electron.*, vol. 13, no. 2, pp. 356–367, 2020, doi: 10.1049/iet-pel.2019.0832.

[32] E. Guerrero-Ramírez, A. Martínez-Barbosa, E. Guzmán-Ramírez, and J. L. Barahona-Ávalos, "Design methodology for digital active disturbance rejection control of the DC motor drive," *e-Prime–Adv. Elect. Eng., Electron. Energy*, vol. 2, Jan. 2022, Art. no. 100050. [Online]. Available: https://www.sciencedirect.com/science/article/pii/S2772671122000225

[33] E. Guerrero-Ramirez, A. Martinez-Barbosa, M. A. Contreras-Ordaz, G. Guerrero-Ramirez, E. Guzman-Ramirez, J. L. Barahona-Avalos, and M. Adam-Medina, "DC motor drive powered by solar photovoltaic energy: An FPGA-based active disturbance rejection control approach," *Energies*, vol. 15, no. 18, Sep. 2022, Art. no. 6595, doi: 10.3390/en15186595.

[34] M. R. Stanković, R. Madonski, S. Shao, and D. Mikluc, "On dealing with harmonic uncertainties in the class of active disturbance rejection controllers," *Int. J. Control*, vol. 94, no. 10, pp. 2795–2810, Mar. 2020, doi: 10.1080/00207179.2020.1736639.

[35] R. Madonski, K. Łakomy, M. Stankovic, S. Shao, J. Yang, and S. Li, "Robust converter-fed motor control based on active rejection of multiple disturbances," *Control Eng. Pract.*, vol. 107, Feb. 2021, Art. no. 104696.

[36] G. K. Srinivasan and H. T. Srinivasan, "Sensorless load torque estimation and passivity based control of Buck converter fed DC motor," *Scientific World J.*, vol. 2015, Mar. 2015, Art. no. 132843. [Online]. Available: https://www.hindawi.com/journals/tswj/2015/132843

[37] G. K. Srinivasan, H. T. Srinivasan, and M. Rivera, "Sensitivity analysis of exact tracking error dynamics passive output control for a flat/partially flat converter systems," *Electron.*, vol. 9, no. 11, Nov. 2020, Art. no. 1942, doi: 10.3390/electronics9111942.

[38] M. G. Kazemi and M. Montazeri, "Fault detection of continuous time linear switched systems using combination of bond graph method and switching observer," *ISA Trans.*, vol. 94, pp. 338–351, Nov. 2019.

[39] J. Yang, H. Wu, L. Hu, and S. Li, "Robust predictive speed regulation of converter-driven DC motors via a discrete-time reduced-order GPIO," *IEEE Trans. Ind. Electron.*, vol. 66, no. 10, pp. 7893–7903, Oct. 2019, doi: 10.1109/TIE.2018.2878119.

[40] R. Silva-Ortigoza, J. N. Alba-Juárez, J. R. García-Sánchez, M. Antonio-Cruz, V. M. Hernández-Guzmán, and H. Taud, "Modeling and experimental validation of a bidirectional DC/DC Buck power electronic converter-DC motor system," *IEEE Latin Amer. Trans.*, vol. 15, no. 6, pp. 1043–1051, Jun. 2017.

[41] R. Silva-Ortigoza, J. N. Alba-Juárez, J. R. García-Sánchez, V. M. Hernández-Guzmán, C. Y. Sosa-Cervantes, and H. Taud, "A sensorless passivity-based control for the DC/DC Buck converter–inverter–DC motor system," *IEEE Latin Amer. Trans.*, vol. 14, no. 10, pp. 4227–4234, Oct. 2016.

[42] E. Hernández-Márquez, J. R. García-Sánchez, R. Silva-Ortigoza, M. Antonio-Cruz, V. M. Hernández-Guzmán, H. Taud, and M. Marcelino-Aranda, "Bidirectional tracking robust controls for a DC/DC Buck converter-DC motor system," *Complexity*, vol. 2018, pp. 1–10, Aug. 2018. [Online]. Available: https://www.hindawi.com/journals/complexity/2018/1260743

[43] X. Chi, S. Quan, J. Chen, Y. X. Wang, and H. He, "Proton exchange membrane fuel cell-powered bidirectional DC motor control based on adaptive sliding-mode technique with neural network estimation," *Int. J. Hydrogen Energy*, vol. 45, no. 39, pp. 20282–20292, 2020.

[44] E. Hernández-Márquez, C. A. Avila-Rea, J. R. García-Sánchez, R. Silva-Ortigoza, M. Marciano-Melchor, M. Marcelino-Aranda, A. Roldán-Caballero, and C. Márquez-Sánchez, "New 'full-bridge Buck inverter–DC motor' system: Steady-state and dynamic analysis and experimental validation," *Electron.*, vol. 8, no. 11, 2019, Art. no. 1216. [Online]. Available: https://www.mdpi.com/2079-9292/8/11/1216

[45] R. Silva-Ortigoza, E. Hernández-Márquez, A. Roldán-Caballero, S. Tavera-Mosqueda, M. Marciano-Melchor, J. R. García-Sánchez, V. M. Hernández-Guzmán, and G. Silva-Ortigoza, "Sensorless tracking control for a 'full-bridge Buck inverter–DC motor' system: Passivity and flatness-based design," *IEEE Access*, vol. 11, pp. 132191–132204, 2021, doi: 10.1109/ACCESS.2021.3112575.

[46] A. A. A. Ismail and A. Elnady, "Advanced drive system for DC motor using multilevel DC/DC Buck converter circuit," *IEEE Access*, vol. 7, pp. 54167–54178, 2019. [Online]. Available: https://ieeexplore.ieee.org/document/8695686

[47] J. Linares-Flores, J. Reger, and H. Sira-Ramírez, "Load torque estimation and passivity-based control of a Boost-converter/DC-motor combination," *IEEE Trans. Control Syst. Technol.*, vol. 18, no. 6, pp. 1398–1405, Nov. 2010.

[48] A. T. Alexandridis and G. C. Konstantopoulos, "Modified PI speed controllers for series-excited DC motors fed by DC-DC Boost converters," *Control Eng. Pract.*, vol. 23, pp. 14–21, Feb. 2014.

[49] S. Malek, "A new nonlinear controller for DC-DC Boost converter fed DC motor," *Int. J. Power Electron.*, vol. 7, nos. 1–2, pp. 54–71, 2015.
[50] G. C. Konstantopoulos and A. T. Alexandridis, "Enhanced control design of simple DC-DC Boost converter-driven DC motors: Analysis and implementation," *Electr. Power Compon. Syst.*, vol. 43, no. 17, pp. 1946–1957, 2015.
[51] P. Mishra, A. Banerjee, M. Ghosh, and C. B. Baladhandautham, "Digital pulse width modulation sampling effect embodied steady-state time-domain modeling of a Boost converter driven permanent magnet DC brushed motor," *Int. Trans. Elect. Energy Syst.*, vol. 31, no. 8, Aug. 2021, Art. no. e12970, doi: 10.1002/2050-7038.12970.
[52] C. T. Manikandan, G. T. Sundarrajan, V. Gokula Krishnan, and I. Ofori, "Performance analysis of two-loop interleaved Boost converter fed PMDC-motor system using FLC," *Math. Problems Eng.*, vol. 2022, Aug. 2022, Art. no. 1639262.
[53] V. H. García-Rodríguez, R. Silva-Ortigoza, E. Hernández-Márquez, J. R. García-Sánchez, and H. Taud, "DC/DC Boost converter-inverter as driver for a DC motor: Modeling and experimental verification," *Energies*, vol. 11, no. 8, pp. 1–15, 2018. [Online]. Available: https://www.mdpi.com/1996-1073/11/8/2044
[54] R. Silva-Ortigoza, V. H. García-Rodríguez, E. Hernández-Márquez, M. Ponce, J. R. García-Sánchez, J. N. Alba-Juárez, G. Silva-Ortigoza, and J. H. Pérez-Cruz, "A trajectory tracking control for a Boost converter–inverter–DC motor combination," *IEEE Latin Amer. Trans.*, vol. 16, no. 4, pp. 1008–1014, Apr. 2018.
[55] J. R. García-Sánchez, E. Hernández-Márquez, J. Ramírez-Morales, M. Marciano-Melchor, M. Marcelino-Aranda, H. Taud, and R. Silva-Ortigoza, "A robust differential flatness-based tracking control for the 'MIMO DC/DC Boost converter–inverter–DC motor' system: Experimental results," *IEEE Access*, vol. 7, pp. 84497–84505, 2019. [Online]. Available: https://ieeexplore.ieee.org/document/8740891
[56] L. N. Egidio, G. S. Deaecto, and R. M. Jungers, "Stabilization of rank-deficient continuous-time switched affine systems," *Automatica*, vol. 143, Sep. 2022, Art. no. 110426.
[57] Y. Sönmez, M. Dursun, U. Güvenç, and C. Yilmaz, "Start up current control of Buck-Boost convertor-fed serial DC motor," *Pamukkale Univ. J. Eng. Sci.*, vol. 15, no. 2, pp. 278–283, 2009.
[58] J. Linares-Flores, J. L. Barahona-Avalos, H. Sira-Ramírez, and M. A. Contreras-Ordaz, "Robust passivity-based control of a Buck–Boost-converter/DC-motor system: An active disturbance rejection approach," *IEEE Trans. Ind. Appl.*, vol. 48, no. 6, pp. 2362–2371, 2012.
[59] E. Hernández-Márquez, R. Silva-Ortigoza, J. R. García-Sánchez, V. H. García-Rodríguez, and J. N. Alba-Juárez, "A new 'DC/DC Buck-Boost converter–DC motor' system: Modeling and experimental validation," *IEEE Latin Amer. Trans.*, vol. 15, no. 11, pp. 2043–2049, Nov. 2017.
[60] E. Hernández-Márquez, R. Silva-Ortigoza, J. R. García-Sánchez, M. Marcelino-Aranda, and G. Saldaña-González, "A DC/DC Buck-Boost converter–inverter–DC motor system: Sensorless passivity-based control," *IEEE Access*, vol. 6, pp. 31486–31492, 2018. [Online]. Available: https://ieeexplore.ieee.org/document/8382160
[61] E. Hernández-Márquez, C. A. Avila-Rea, J. R. García-Sánchez, R. Silva-Ortigoza, G. Silva-Ortigoza, H. Taud, and M. Marcelino-Aranda, "Robust tracking controller for a DC/DC Buck-Boost converter–inverter–DC motor system," *Energies*, vol. 11, no. 10, 2018, Art. no. 2500. [Online]. Available: https://www.mdpi.com/1996-1073/11/10/2500
[62] M. R. Ghazali, M. A. Ahmad, and R. M. T. R. Ismail, "Adaptive safe experimentation dynamics for data-driven neuroendocrine-PID control of MIMO systems," *IETE J. Res.*, vol. 68, no. 3, pp. 1611–1624, 2019.
[63] J. Linares-Flores, H. Sira-Ramírez, E. F. Cuevas-López, and M. A. Contreras-Ordaz, "Sensorless passivity based control of a DC motor via a solar powered Sepic converter-full bridge combination," *J. Power Electron.*, vol. 11, no. 5, pp. 743–750, Sep. 2011.
[64] M. Vanitha and D. Murali, "Applied voltage control scheme for a DC motor fed by a Sepic based DC-DC converter," *Int. J. Innov. Sci. Res. Technol.*, vol. 6, no. 12, pp. 785–789, 2021.
[65] E. E. Jiménez-Toribio, A. A. Labour-Castro, F. Muñiz-Rodríguez, H. R. Pérez-Hernández, and E. I. Ortiz-Rivera, "Sensorless control of Sepic and Ćuk converters for DC motors using solar panels," in *Proc. IEEE Int. Electr. Mach. Drives Conf.*, Miami, FL, USA, May 2009, pp. 1503–1510.
[66] M. H. Arshad and M. A. Abido, "Hierarchical control of DC motor coupled with Cuk converter combining differential flatness and sliding mode control," *Arabian J. Sci. Eng.*, vol. 46, no. 10, pp. 9413–9422, Oct. 2021, doi: 10.1007/s13369-020-05305-9.
[67] G. K. Srinivasan, H. T. Srinivasan, and M. Rivera, "Low-cost implementation of passivity-based control and estimation of load torque for a Luo converter with dynamic load," *Electron.*, vol. 9, no. 11, Nov. 2020, Art. no. 1914, doi: 10.3390/electronics9111914.
[68] H. Sira-Ramírez and R. Silva-Ortigoza, *Control Design Techniques in Power Electronics Devices*, 1st ed. London, U.K.: Springer-Verlag, 2006.
[69] L. Gil-Antonio, B. Saldivar, O. Portillo-Rodríguez, G. Vázquez-Guzmán, and S. M. De Oca-Armeaga, "Trajectory tracking control for a Boost converter based on the differential flatness property," *IEEE Access*, vol. 7, pp. 63437–63446, 2019. [Online]. Available: https://ieeexplore.ieee.org/document/8713460
[70] H. Sira-Ramírez, "Flatness and trajectory tracking in sliding mode based regulation of DC-to-AC conversion schemes," in *Proc. 38th IEEE Conf. Decis. Control*, Phoenix, AZ, USA, Dec. 1999, pp. 4268–4273, doi: 10.1109/CDC.1999.833212.
[71] E. Hernández-Márquez, R. Silva-Ortigoza, H. Taud, G. Saldaña-González, and M. Marcelino-Aranda, "New mathematical models for the DC/DC Boost converter," in *Proc. Int. Conf. Mechatronics, Electron. Automot. Eng. (ICMEAE)*, Morelos, Mexico, Nov. 2018, pp. 157–160.
[72] R. Kumar and B. Singh, "BLDC motor-driven solar PV array-fed water pumping system employing Zeta converter," *IEEE Trans. Ind. Appl.*, vol. 52, no. 3, pp. 2315–2322, May 2016, doi: 10.1109/TIA.2016.2522943.
[73] R. Kumar and B. Singh, "Single stage solar PV fed brushless DC motor driven water pump," *IEEE J. Emerg. Sel. Topics Power Electron.*, vol. 5, no. 3, pp. 1377–1385, Sep. 2017, doi: 10.1109/JESTPE.2017.2699918.
[74] J. J. Tafoya-Sánchez, "Control de velocidad angular de motores de corriente directa mediante técnicas de control automático," Ph.D. dissertation, Instituto Politécnico Nacional, Mexico City, Mexico, Dec. 2010.

RAMÓN SILVA-ORTIGOZA (Member, IEEE) received the B.S. degree in electronics from Benemérita Universidad Autónoma de Puebla (BUAP), Puebla, Mexico, in 1999, and the M.S. and Ph.D. degrees in electrical engineering from the Centro de Investigación y Estudios Avanzados del Instituto Politécnico Nacional (CINVESTAV-IPN), Mexico City, Mexico, in 2002 and 2006, respectively, with a focus on mechatronics.

He has been a Researcher with the Department of Mechatronics and Renewable Energy, Centro de Innovación y Desarrollo Tecnológico en Cómputo, IPN (CIDETEC-IPN), since 2006, and belongs to SNI-CONACYT, Mexico. He has coauthored books, such as *Control Design Techniques in Power Electronics Devices* (Power Systems Series; London, U.K.: Springer-Verlag, 2006), *Automatic Control: Design Theory, Prototype Construction, Modeling, Identification and Experimental Tests* (in Spanish; Mexico City, MX: CIDETEC-IPN, 2013), *Automatic Control with Experiments* (Advanced Textbooks in Control and Signal Processing Series; Cham, Switzerland: Springer Nature, 2019), and *Energy-Based Control of Electromechanical Systems: A Novel Passivity-Based Approach* (Advances in Industrial Control Series; Cham, Switzerland: Springer Nature, 2021). He has published more than 70 articles in JCR-indexed journals, 50 works in scientific divulgation journals and bulletins, and three chapters in international books. He has presented more than 45 papers at international conferences. He has been an advisor to more than 35 postgraduate students and four B.S. students. He has been the leader of more than 15 research projects and collaborated on ten additional research projects. His research work has been cited more than 1300 times. He has been a reviewer of several JCR-indexed journals. His research interests include mechatronic control systems, mobile robotics, control in power electronics, renewable energy, AC and DC motors, the development of educational technology, and mathematical physics.

Dr. Silva-Ortigoza has been a referee in several awards of research and engineering, the National Program of Quality Postgraduate, and research projects of CONACYT. Six of his students have been honored with the Presea Lázaro Cárdenas Award, in 2012, 2015, 2016, 2018, 2019, and 2020, the most important prize granted by the Instituto Politécnico Nacional of Mexico to its students. Three of these students have also been honored with the Best Postgraduate Thesis Award by the Instituto Politécnico Nacional of Mexico, in 2015, 2017, and 2020. He was an Editor of the book *Mechatronics* (in Spanish; Mexico City, Mexico: CIDETEC-IPN, 2010).

ALFREDO ROLDÁN-CABALLERO received the B.S. degree in mechatronics from BUAP, Puebla, Mexico, in 2013, the M.S. degree in manufacture from Sección de Estudios de Posgrado e Investigación, Escuela Superior de Ingeniería Mecánica y Eléctrica del Instituto Politécnico Nacional (ESIME-IPN), Mexico City, Mexico, in 2016, and the Ph.D. degree in engineering of robotic and mechatronic systems from CIDETEC-IPN, Mexico City, in 2021.

He is currently a Professor with Unidad Profesional Interdisciplinaria de Ingeniería Campus Tlaxcala del Instituto Politécnico Nacional. His research interests include the theory and application of automatic control in mechatronics systems, mobile robots, power electronics, and renewable energy.

EDUARDO HERNÁNDEZ-MÁRQUEZ (Member, IEEE) received the B.S. degree in electromechanical from Instituto Tecnológico Superior de Poza Rica, Veracruz, Mexico, in 2005, the M.S. degree in automatic control from CINVESTAV-IPN, Mexico City, Mexico, in 2008, and the Ph.D. degree in engineering of robotic and mechatronic systems from CIDETEC-IPN, Mexico City, in 2019.

Since 2008, he has been a Research Professor with Instituto Tecnológico Superior de Poza Rica and belongs to SNI-CONACYT, Mexico, with Level I. His research interests include the theory and application of automatic control in mobile robotics, disturbance rejection, and power electronic systems.

ROGELIO ERNESTO GARCÍA-CHÁVEZ received the B.S. degree in informatics engineering from Unidad Profesional Interdisciplinaria de Ingeniería y Ciencias Sociales y Administrativas del Instituto Politécnico Nacional (UPIICSA-IPN), Mexico City, Mexico, in 2022. He is currently pursuing the M.S. degree with the Department of Mechatronics and Renewable Energy, CIDETEC-IPN.

His research interests include the theory and application of automatic control in power electronic systems and mobile robotics.

MAGDALENA MARCIANO-MELCHOR received the B.S., M.S., and Ph.D. degrees in mathematics from Benemérita Universidad Autónoma de Puebla, Puebla, Mexico, in 1999, 2002, and 2006, respectively.

She has been a Professor and a Researcher with CIDETEC-IPN, since 2007. She has been an Advisor to several postgraduate students and the Leader of research projects with IPN. She belongs to SNI-CONACYT, Mexico, and the Mexican Societies of Physics and Mathematics. She has published several articles in JCR-indexed journals. Her research interests include dynamic systems, control theory, and mathematical physics.

JOSÉ RAFAEL GARCÍA-SÁNCHEZ received the B.S. degree in industrial robotics from ESIME-IPN, Mexico City, Mexico, in 2003, the M.S. degree in automatic control from Universidad Nacional Autónoma de México, Mexico City, in 2013, and the Ph.D. degree in engineering of robotic and mechatronic systems from CIDETEC-IPN, Mexico City, in 2018.

He is currently a Professor and a Researcher with the Department of Mechatronics, Tecnológico de Estudios Superiores de Huixquilucan, Tecnológico Nacional de México, and belongs to SNI-CONACYT, Mexico. He has published and presented papers in JCR-indexed journals and international conferences, respectively. His research interests include the theory and application of automatic control in mobile robotics, teleoperated systems, and power electronic systems. During his academic trajectory, he was a recipient of the Distinction to Polytechnic Merit: Presea Lázaro Cárdenas in the physical and mathematical sciences area at the Ph.D. level, in 2018.

GILBERTO SILVA-ORTIGOZA received the B.S. degree in physics from BUAP, Puebla, Mexico, in 1988, and the M.S. and Ph.D. degrees in physics from CINVESTAV-IPN, Mexico City, Mexico, in 1991 and 1995, respectively.

He has been a Professor and a Researcher with the Facultad de Ciencias Físico Matemáticas, BUAP, since 1991, and belongs to SNI-CONACYT, Mexico, with Level II. He has published more than 80 articles in journals indexed in Journal Citation Reports. His research interests include general relativity, geometrical optics, and the mathematical modeling of dynamical systems.